Hendy Ingrid (Orcid ID: 0000-0001-8305-6752)

Assessing oxygen depletion in the Northeastern Pacific Ocean during the last deglaciation using I/Ca ratios from multiple benthic foraminiferal species

M.A. Taylor[a,b], I.L. Hendy[b], A. Chappaz[c]

[a] Ecosystem Center for Science and Society, Northern Arizona University, Flagstaff, AZ 86011

[b] Department of Earth and Environmental Sciences, University of Michigan, Ann Arbor, MI 48109

[c] Department of Earth and Atmospheric Science, Central Michigan University, Mount Pleasant, MI 48859

Corresponding author: meghan.taylor@nau.edu,

phone: 313-550-5357, fax: 734-763-4690

KEY POINTS

- Three benthic foraminifera species show expected I/Ca ratios in Northeast Pacific core record relative to their depth habitat.
- Foraminiferal I/Ca-based O_2 reconstructions are supported by multiple proxies in the same sediment samples

This is the author manuscript accepted for publication and has undergone full peer review but has not been through the copyediting, typesetting, pagination and proofreading process, which may lead to differences between this version and the Version of Record. Please cite this article as doi: 10.1002/2016PA003062

- Oxidant demand was greatest during the Bølling; pore and bottom waters were most oxygenated during the Younger Dryas and last glacial.

ABSTRACT

Paleo-redox proxies are crucial for reconstructing past bottom water oxygen concentration changes brought about by ocean circulation and marine productivity shifts in response to climate forcing. Carbonate I/Ca ratios of multiple benthic foraminifera species from ODP Hole 1017E – a core drilled within the Californian oxygen minimum zone (OMZ), on the continental slope – are employed to re-examine the transition from the well oxygenated last glacial into poorly oxygenated modern conditions. The redox and export productivity history of this site is constrained by numerous proxies, used to assess sensitivity of I/Ca ratios of benthic foraminifera to changes in bottom- and pore water O_2 concentrations. Reconstructed iodate (IO_3^-) availability from the I/Ca ratio of epifaunal (*Cibicidoides* sp.), shallow infaunal (*Uvigerina peregrina*), and deep infaunal (*Bolivina spissa*) foraminifera. The reconstructed IO_3^- availability profile is used to determine the contribution of bottom water O_2 relative to oxidant demand on pore water O_2 concentrations. These results suggest that high export productivity on the California Margin drove pore low water O_2 concentrations during the Bølling. In contrast low bottom water O_2 concentrations at 950 m water depth only contributed to reduced

sediments during the Allerød. Increased contribution of modified North Pacific Intermediate Water to the California Current System ventilated the California OMZ during the late glacial and the Younger Dryas such that water overlying the site was oxygenated. These results highlight the promising potential of this new proxy for understanding the relative influence of bottom water O_2 concentration and pore water oxidant demand on OMZs.

1. INTRODUCTION

Recent monitoring of dissolved oxygen (O_2) concentrations has highlighted the increasing volume of O_2-depleted intermediate waters in the oceans over the last few decades (Whitney et al., 2007; Diaz and Rosenberg, 2008; Keeling et al., 2010). The oxygen minimum zone (OMZ) in Eastern Tropical Pacific (ETP) has expanded vertically by 85% from 1960-2006 and model projections predict further O_2 loss (Stramma et al., 2008). An intensified OMZ within the California Current System in the northeast Pacific Ocean has been associated with warmer waters and abrupt climate shifts over millennial time scales (Cannariato and Kennett, 1999; Hendy et al., 2004; Ohkushi et al., 2013; Moffit et al., 2014, Tetard et al., 2017). Given OMZ sensitivity to climate change, and the decrease in the diversity and density of benthic fauna below ~20 umol kg^{-1} of O_2 (Levin, 2003), predicting how global warming-triggered O_2 loss would affect marine ecosystems is critical.

Iodine has become a promising indicator of O_2 depleted conditions because the iodide/iodate redox potential is close to that of O_2/H_2O (Rue et al., 1997). In oxygenated water, dissolved I is present as iodate $I(+V)O_3^-$, the dominant and thermodynamically stable form of iodine. As O_2 concentrations in water decrease, IO_3^- is reduced to iodide I^- (-1) such that I^- is the dominant and thermodynamically stable species in anoxic seawater (Rue et al., 1997; Chapman and Truesdale, 2011). Iodine displays a nutrient-like vertical distribution in seawater (Elderfield and Truesday, 1980) as iodine accumulates in marine plankton and sinking organic particles. Diagenesis of iodine occurs when early sedimentary degradation of labile high molecular weight organic matter releases iodine to porewaters in the reduced form (I^-), which in the presence of O_2, is slowly oxidized to IO_3^- (Kennedy and Elderfield, 1987).

In calcite, IO_3^- substitutes for carbonate anions proportionately to the IO_3^- concentration of the surrounding water. Synthesized carbonate minerals take up IO_3^- linearly with concentration indicating that biogenic carbonate I/Ca ratios would be suitable as a quantitative proxy for detecting IO_3^- availability as bottom water O_2 changes assuming analogous behavior between inorganic and biogenic precipitates. Measuring I/Ca ratios in carbonate forming organisms such as foraminifera has been proposed to estimate potential O_2 depleted conditions in ancient oceans (Lu et al., 2010). A similar approach, consisting of determining bulk carbonate or planktonic and benthic foraminiferal I/Ca ratios, has been applied to ocean oxygenation events such as the

Precambrian Great Oxidation Event and Mesozoic Oceanic Anoxic Events (Hardisty et al., 2014, 2017; Zhou et al., 2014, 2015, 2016).

Currently, there are limited calibrations of modern benthic foraminiferal calcite available, limiting the potential of I/Ca ratios in foraminifera as a quantitative proxy for past O_2 depleted conditions. Positive linear correlations were identified within the Peruvian Margin OMZ between benthic species-specific foraminiferal I/Ca and a narrow range of bottom water O_2 concentrations (2-35 µM kg^{-1}) (Glock et al., 2014; Glock et al., 2016). However, benthic species of the same genus and similar depth habitats may have differing sensitivities to the I/Ca-[O_2] relationship as vital effects also influence IO_3^- uptake (Glock et al., 2014). Although there remains a need for species-specific calibration, the developing I/Ca redox proxy has the ability to provide information about dynamic O_2 concentrations in ancient marine systems.

The mechanisms driving changes in North Pacific OMZs during the last deglacial are not well understood. The hypothesized environmental regulators of bottom and pore water O_2 concentrations are not mutually exclusive and include changes in primary productivity (both regional and far-field), and ocean circulation that affects intermediate water ventilation. Iodine/Ca ratios of benthic foraminifera from ODP Hole 1017E on the California Margin were measured to explore the sensitivity of I/Ca ratios of different species to O_2 depletion in their environment. We compare our results with previous OMZ reconstructions within the same core that identified redox driven metal enrichments

(Hendy and Pederson, 2005) O_2 sensitive and benthic foraminiferal assemblages (Cannariato and Kennett, 1999) already exist to confirm the veracity of the new proxy. Our study demonstrates the potential application of I/Ca in benthic foraminifera and is a first step in establishing this paleo-redox proxy as an efficient "tool" capable of determining past O_2 depleted conditions in sediment and pore water environments.

2. BACKGROUND

Site description

ODP Hole 1017E (34°32 N; 121°60 W; 955 m water depth) is located near the base of the modern California margin OMZ (Fig. 1A). The strength of the California OMZ is tightly coupled to upwelling and water masses advected into the region. A persistent coastal upwelling cell is located above the site, as the geometry and high-relief of the coastline accelerates airflow, from northerly winds associated with the strengthening and poleward moving North Pacific high pressure cell in early spring (Lynn and Simpson, 1987). The site is bathed by modified North Pacific Intermediate Water (NPIW) transformed during gyral circulation, where mixing with multiple subsurface water masses occurs. NPIW is oxygenated by two subarctic sources - the Okhotsk Sea and the Gulf of Alaska (You, 2003). These intermediate waters are mixed via cabbeling – a process that mixes distinctly different water masses to produce a higher density water mass – during transit across the North Pacific before entering the

subtropical gyre. The loss of defined NPIW characteristics (i.e. salinity minimum between 33.9 – 34.4 ‰ or density of $\sigma\theta = 26.8$; Auad et al., 2003) prevents direct association with NPIW and therefore we refer to the water bathing the California Margin at intermediate water depths as modified NPIW. Modified NPIW is mixed with the California Current System (CCS) on the margin by eddy activity such that it is integral to the current system. Additionally, poleward flow mostly at ~200-300 m water depth transports poorly oxygenated warm, salty water from the Eastern Tropical North Pacific (ETNP) inshore of the CCS via the California Undercurrent (CU) (Noble and Ramp, 2000, Nam et al., 2015). The core of CU contains water formed from deep winter mixed layers between 25–30°N, and 130–140°W (Hautala and Roemmich, 1998). Upwelling then brings this water from 200 – 300 m depth into the photic zone.

Low O_2 concentrations in OMZs result from the decomposition of organic matter by microbial activity that consumes dissolved O_2. A NE Pacific transect of dissolved O_2 concentrations in the water column demonstrates that the core site is presently bathed by water with O_2 concentration of ~25µmol kg^{-1} (Fig. 1B). In water depths ranging from ~580 – 4,000 m, dissolved O_2 in pore waters off of central California became anoxic at >0.4-3 cm below the sediment water interface (SWI) (Reimers et al., 1992). At the measuring stations within the OMZ, dissolved O_2 is undetectable (<15 µmol kg^{-1}) between 4-7 mm below the SWI (Reimers et al., 1987; 1992). Pore water O_2 concentrations increase outside the OMZ: O_2 is < 60 µmol kg^{-1} at 6-16 mm below the

SWI on the lower slope and > 100 µmol kg^{-1} at 10-30 mm on the continental rise (Reimers et al., 1987; 1992).

Iodate availability should follow the O_2 water column profile of dissolved O_2 concentration. Measurements of dissolved O_2 in water column profiles from the ETP reveal sharp IO_3^- and I^- gradients where reduction of IO_3^- to I^- occurs between 140-600 m, defining an OMZ (O_2 < 5µmol kg^{-1}) that is maintained to a depth of ~900 m (Rue et al., 1997).

3. METHODS

3.1 Radiocarbon age model and core chronology

The age model for ODP Hole 1017E is based upon 11 ^{14}C dates from the upper 4.70 m of the core (Hendy et al., 2004) calibrated to calendar years. The original chronology for the core has been modified using the MARINE13 calibration (Reimer et al., 2013) generating a new calendar year based chronology through the deglacial interval (Fig. S1 and Table S1). A constant regional reservoir correction (ΔR) of 402.7 ±50 years was assumed (Robinson and Thompson, 1981).

3.2 Analysis of I and Ca contents in foraminiferal species

Samples were picked at continuous intervals from 2.52 to 4.20 m (corrected) below core top in ODP Hole 1017E where sufficient specimens were available. Benthic species investigated for I/Ca were selected using several criteria. Sufficient populations

of each species down core were necessary for a meaningful interspecies comparison. Additionally, species were chosen that are relatively ubiquitous, live across a range of depth habitats and are commonly used in paleoclimate reconstructions. The suspension feeding *Cibicidoides sp.* are epifaunal, living on objects above the SWI (Altenbach and Sarnthein, 1989), while *Uvigerina* and *Bolivina* are both infaunal, cylindrical species associated with high food supply and/or low O_2. Approximately 3 individual infaunal *Uvigerina peregrina* (shallow infaunal, low O_2 indicator), 25 *Bolivina spissa* (deep infaunal, low O_2 indicator), and 3 epifaunal *Cibicidoides sp.* (an oxic indicator) respectively were used to achieve a sample weight of ~300 μg for each analysis (Cannariato and Kennett, 1999). *U. peregrina* dominates assemblages in the upper and lower bounds of the OMZ (Cannariato and Kennett, 1999). Gaps in the record occur when insufficient specimens were available for analysis. Recent high-resolution secondary ion mass-spectrometry analyses of individual foraminiferal tests from the Peruvian margin suggest intra-test variability of I/Ca ratios (Glock et al., 2016). Therefore in future work it may be advisable to conduct bulk ICP-MS analyses of larger pools of individuals.

All chemical analyses were carried out under ultra-clean conditions for iodine and Ca using a Thermo iCAPq quadrupole ICP-MS at the STARLAB (Central Michigan University) (Table 2) (Lu et al., 2010; Glock et al., 2014). Visual inspection prior to analysis confirmed that foraminifera were well preserved. Samples were weighed and

crushed prior to undergoing cleaning of contaminant phases via a multi-step protocol involving clay removal, and oxidative cleaning steps. (Martin and Lea, 2002). Samples were dissolved into 0.075 M HNO_3 and spiked with yttrium (internal standard). Tetramethyl ammonium hydroxide (TMAH, 25% in H_2O, Trace-SELECT, impurities: ≤ 10 $\mu g kg^{-1}$ total iodine, Sigma Aldrich^{TM}) was added to every sample to reduce loss of iodine due to volatilization (no headspace). A micro-nebulizer was used to inject the small volumes of solution prepared (300 – 500 µL). For the preparation of standards, 25 mg solid KIO_3 (suprapure, Sigma Aldrich^{TM}) were dissolved with 15 mL ultrapure water, 25% TMAH, HNO_3, and spiked with Ca, and Y. These solutions were diluted to prepare working standards via pre-dilution (Table 1), and were prepared fresh daily. Standards were run between every 10 – 15 samples. All I/Ca ratios are reported in µmol, mol^{-1} henceforth. Samples were analyzed (three scans) directly after acidification to prevent loss of volatile iodine because although TMAH traps iodine, significant volatilization occurs within 24 hours (Glock et al., 2014). For a small number of samples (12, marked with a * symbol in Table 2), we discarded the last and third measurement that was significantly different from the first two measurements. These divergences could be attributed to the very small volume of solution available for analysis. For these 12 samples, we suspect all the solution was consumed before the end of the third run. The average relative standard deviation was equal to 5.7±4.2 %; a reasonable range of values considering a micro-nebulizer was used. The detection limit for iodine was 5 ppt.

Detailed information the quality of our measurements (e.g. blank CPS, standards CPS, calibration curves, internal standard recovery, quality controls) are provided (Table S2 and S3; Figure S2). The analytical precision for I/Ca splits (7 pairs, 2 *Cibicidoides sp.* 2 *B. spissa*, 3 *U. peregrina*), reflecting both analytical and sample-processing uncertainty is 0.20 µmol/mol (1 σ).

Previous studies focusing on the development of the I/Ca proxy in foraminifera used a reference material (JCp-1, coral standard) (Lu et al., 2010; Glock et al., 2014; Hardisty et al. 2014, 2017; Zhou et al., 2014, 2015, 2016). When designing our analytical plan, we did not include this reference material within our study because it is not certified for iodine. We realize our choice may be questionable. Although this omission does not challenge our data quality (see supporting information), we acknowledge we should have included JCp-1 to allow an easier comparison with these previous studies. For this work, it was too late to incorporate JCp-1 but we strongly recommend that any future I/Ca study do so.

4. RESULTS

All three species of benthic foraminifera broadly exhibit the same I/Ca trends throughout the core record (Fig. 2). I/Ca ratios were high during the Last Glacial Maximum (LGM), relative to the Bølling/Allerød (B/A) warming. Data from all species

are sparse during the Younger Dryas (YD) with the exception of *Cibicidoides sp.* that records similar values as the LGM (Fig. 2A). The highest I/Ca ratios (ave = 7.53 in the YD and 7.19 during the LGM or 0.8-3.5 µmol mol^{-1}) were measured in the epifaunal *Cibicidoides sp.*, reflecting the highest bottom water O_2 concentrations. Ratios dropped (ave = 5.75) during the Bølling and decreased further to an average of 3.02 during the Allerød. These values are similar to although wider in range than I/Ca measured in epifaunal *P. limbata* (1.03-2.2 µmol mol^{-1}), which exhibited the greater I/Ca range in a modern study of an O_2 concentration gradient (~5-25 µmol L^{-1}) through the Peruvian OMZ (Glock et al., 2014). Measured I/Ca ratios of *B. spissa*, were lower and less variable (0.05-1.5 µmol mol^{-1}), reflecting the O_2 depleted pore waters of the deeper infaunal habitat of this species (Fig. 2C). One *B. spissa* datum was significantly higher than the rest of the data set (>3sd) and was discarded as an outlier, but is reported in Table 2 (denoted by **). *B. spissa* recorded average I/Ca values of 1.95 during the LGM and 2.05 during the YD. In contrast to *Cibicidoides, B. spissa* recorded the lowest I/Ca values (ave = 0.59) during the Bølling with slightly higher values during the Allerød (ave = 1.09). The I/Ca values of shallow infaunal species *U. peregrina* generally fell between the epifaunal and deep infaunal species (average I/Ca ratio of 0.57-3.96 or 0.08-3.1 µmol mol^{-1}) (Fig. 2B). These values are also similar yet wider ranging than the I/Ca measured in the shallow infaunal *U. striata* (0.31-0.91 µmol mol^{-1}) on the Peru Margin (Glock et al., 2014). *Uvigerina* recorded high average I/Ca values (ave = 3.96) during the LGM.

Similar to the deep infaunal species, the lowest values (ave = 0.57) were recorded during the Bølling, before increasing to an average of 1.44 during the Allerød. That the foraminiferal I/Ca values at ODP Hole 1017E during the LGM display a such a large range should be anticipated as the site is known to transition from well oxygenated to O_2 depleted conditions during deglaciation. The modern study, on the other hand, was restricted in time to the modern Peru Margin OMZ. However, the I/Ca ratios from the modern study can be used to infer upper bounds on suboxic I/Ca ratios for these species based on the range of O_2 concentrations measured.

5. DISCUSSION

5.1 Reconstructing past iodate (IO_3^-) availability in bottom and pore waters

Benthic species selected for this study are widely used in paleoclimate reconstructions. They appear to be responsive to past changes in water column and pore water oxygenation, suggesting that they are good candidates for further modern calibration studies. Despite potentially confounding species-specific factors, all benthic foraminiferal species capture similarly robust trends in I/Ca in the downcore record indicating IO_3^- availability in bottom and pore water has changed through time at ODP Hole 1017E (Fig. 2).

Epifaunal and infaunal benthic foraminiferal I/Ca ratios enable reconstruction of IO_3^- availability from the different sediment depths inhabited by the foraminifera (Fig. 3)

as only IO_3^- is incorporated into the foraminiferal carbonate. The O_2 level present at the SWI influences the type of diagenetic reactions occurring within the first centimeters, based on the redox sequence (Middleburg and Levin, 2009). These processes control iodine pore water chemistry in the ~10 cm below the SWI as reduced iodine is released to pore waters by decomposition of labile organic matter and oxidizes to IO_3^- only if O_2 is present. (Kennedy and Elderfield, 1987). Foraminiferal species living within this sediment interval are exposed to changing IO_3^-/I^- ratios. I/Ca ratios from epifaunal, and shallow-to-deep infaunal benthic foraminifera therefore reproduce an IO_3^- availability gradient that tracks O_2 concentration from the SWI to pore waters.

In fully oxygenated overlying water, iodine present as IO_3^- (Middleburg and Levin, 2009) allows epifaunal benthic foraminifera to record high I/Ca ratios such as occurred during the LGM (Fig 3B) and Bølling (Fig 3C). Near the SWI, I^- released by degradation of labile organic matter through microbial activity, is oxidized in pore waters and released to bottom waters (Francois, 1987; Kennedy and Elderfield, 1987; Price and Calvert, 1973). Increased oxidant demand decreases pore water O_2 concentrations and I^- oxidation becomes unfavorable causing decreased IO_3^- concentration in pore waters. Thus, deep infaunal species have lower I/Ca ratios than shallow species (Fig 2 and Figs 3B and 3C). As the IO_3^-/I^- gradient declines rapidly in C_{org}-rich sediments, the I/Ca ratio of deep infaunal species will be significantly lower than epifaunal species such as occurred during the Bølling (Fig. 3C). Under low bottom water O_2 conditions, I^- released

by organic matter degradation at the SWI is not oxidized and the decreased IO_3^-/I^- ratio in bottom water results in a low epifaunal I/Ca such as occurred during the Allerød (Fig. 3D). Following the TRophic conditions and OXygen (TROX) model (Jorissen et al., 1995) infaunal species may migrate to the SWI following food availability in an oligotrophic environment such as shown in the oxic water scenario (Fig 3A). However, in the eutrophic coastal upwelling environment of ODP Hole 1017E O_2 concentration preferences determine the penetration depth of infaunal species.

The IO_3^- availability change through time at ODP Hole 1017E can also be observed in bulk sediment I/Br ratios (Hendy and Pedersen, 2005). Sedimentary I/Br ratios are diagenetically altered by loss of iodine from organic labile organic matter relative to Br (Price and Calvert, 1973; Price and Calvert, 1977; Francois, 1987). Under suboxic and anoxic conditions, iodine in sediments is typically depleted relative to Br as the reduced I^- ion is lost from labile high molecular weight organic matter, while the Br^- ion remains regardless of redox conditions (Price and Calvert, 1977). Low sedimentary IO_3^- availability dominates the ODP Hole 1017E record as indicated by the persistently low bulk sediment I/Br ratios. Exceptions occurred between 17.5 -15 ka (Heinrich 1) and 12-10.5 ka (YD) (Fig. 4B) indicating higher IO_3^- availability in sediments and therefore higher pore water O_2 concentrations. These results demonstrate the potential of I/Ca as a paleo-redox proxy.

5.2 Multiple proxy comparison at core site OPD-1017E

Previously published benthic foraminiferal assemblages and redox sensitive metal enrichments measured in the same ODP-Hole 1017E sediment samples (Cannariato and Kennett, 1999; Hendy et al., 2004; Hendy and Pedersen, 2005) support I/Ca-based IO_3^- availability profiles presented here. We compare these proxy records with previously published ODP-1017E $\delta^{15}N$ values and C_{org} concentrations, which are related to export production at the site, driven both by physical (i.e. wind driven coastal upwelling) and biogeochemical processes (i.e. nutrient availability in upwelled water) (Cannariato and Kennett, 1999; Hendy et al., 2004; Hendy and Pedersen, 2005) (Fig. 4 and 5). Bulk sediment $\delta^{15}N$ at this site is interpreted to be a regional signature where nitrate is enriched in ^{15}N through denitrification in the ETNP, and transported northward via the CU (Hendy et al., 2004; Hendy et al., 2006; Pichevin et al., 2010, Kienast et al., 2002). Thus high values indicate upwelled water was sourced from a region of denitrification (ETNP), while low values indicate either upwelling ceased, and/or that shallow subsurface waters were oxygenated (Hendy et al, 2004; Kienast et al., 2002).

Multiple proxies suggest that during the LGM bottom waters at 950 m water depth were oxic, pore waters were suboxic, and export production was relatively low at ODP-1017E. High epifaunal (*Cibicidoides sp.*) I/Ca values indicate relatively oxic conditions in bottom waters, as does the relative abundance of oxic (O_2 = >67 µmol kg^{-1}) benthic foraminiferal species that varies between 10-30% (Cannariato and Kennett, 1999) (Fig. 4F). Both the epifaunal and shallow infaunal (*U. peregrina*) I/Ca values are more

variable during this interval, apparently affected by sedimentary events. Thin sand layers deposited by downslope processes during sea level minima (Tada et al., 2000) coincide with the highest I/Ca values below the SWI prior to ~17.5 ka.

During the LGM deep infaunal (*B. spissa*) I/Ca values remain lower in pore waters than epifaunal *Cibicidoides* values and benthic assemblages are dominated (~50%) by suboxic (defined as O_2 = ~13.5-67 µmol kg^{-1}) infaunal species (Fig. 2; Cannariato and Kennett, 1999). At ~18 ka, Re enrichments of 5 to 18 ppb (Hendy and Pedersen, 2005) support sedimentary suboxia, indicating O_2 depletion in pore waters (Crusius et al., 1996) (Fig. 4C). Sedimentary Re enrichments have been proposed as an indicator of suboxic conditions (Crusius et al., 1996), although burial might be controlled by precipitation of Re-sulfur phases at the SWI (Chappaz et al., 2008, Helz and Dolor, 2012).

Oxidant demand in sedimentary pore waters was not large during the LGM as export productivity was relatively low. Delivered to sediments by organic matter, Cd and Ag precipitate in anoxic sediments as insoluble CdS (Rosenthal et al., 1995) and Ag_2S (Dyrssen and Kremling, 1990) when trace amounts of pore water sulfide are present (Wagner et al., 2013; Wagner et al, 2015). During the LGM low concentrations of redox sensitive Cd (1000 ppb) and Ag (200 ppb) have been interpreted to reflect reduced delivery of biogenic sediments (Fig 5D-E; Hendy et al., 2004). Organic carbon content was relatively low (~1.5% during this interval with lower values also associated with the

thin sand layers (Tada et al., 2000) (Fig. 5C). These results support the relatively high infaunal I/Ca ratios indicating oxygenated pore waters due to a relatively low oxidant demand.

Low bulk sediment $\delta^{15}N$ during the LGM is interpreted to represent better-ventilated water in the CU at ~300 m water depth (Fig. 5B, Hendy et al., 2004). Although in the ETNP $\delta^{15}N$ and redox-sensitive metal concentrations increase at ~17 ka (prior to the Bølling) suggesting OMZ expansion (Hendy and Petersen, 2006), values of these proxies remain low on the California Margin (Hendy and Pedersen, 2005). This has been taken to indicate minimal poleward transport of low O_2, denitrified ETNP water by the CU and increased O_2 within modified NPIW on the North American Margin (Hendy and Pedersen, 2005; Chang et al., 2008; 2014). These observations support high epifaunal I/Ca ratios indicating oxygenated bottom waters.

During the Bølling warming at 14.7 ka the ratio of warm water (>12°C) dextral to cool water (<10°C) sinistral *N. pachyderma* increased to >80% (Fig. 5A). Epifaunal I/Ca ratios remained high implying that oxygenated bottom waters (~950 m water depth) persisted at ODP Hole 1017E, however, shallow-to-deep infaunal I/Ca decreased abruptly indicating the pore water O_2 concentrations dropped. An increase in relative abundance (30-50%) of dysoxic (O_2 = ~4.5-13.5 μmol kg^{-1}) benthic foraminiferal species supports the low pore water oxygenation suggested by infaunal I/Ca ratios. The remaining 5-30%

relative abundance of oxic benthic foraminifera supports the high epifaunal I/Ca ratios that indicate oxic bottom waters (Fig. 4; Cannariato and Kennett, 1999).

Trace metal enrichments suggest pore waters were sulfidic during the Bølling (Fig. 3). Molybdenum enrichment is a proxy for sulfidic conditions (Chappaz et al., 2014, in press) in sediments. Molybdenum concentrations increased, (Hendy and Peterson, 2005) but did not exceed 10 ppm, indicating free dissolved sulfide and thiomolybdates were present but restricted to pore waters (Scott and Lyons, 2012) (Fig. 4D). A decrease in the Re/Mo ratio mirrors this increase in pore water sulfide, as Re remains low under high sulfide concentrations (Hendy and Pedersen, 2005) (Fig. 4C & 4E). The I/Br ratio of bulk sediments dropped from 1.5 to 0.5 indicating a loss of IO_3^- from organic matter in sediments as pore water O_2 concentrations dropped (Hendy and Pedersen, 2005) consistent with the low I/Ca ratios of infaunal benthic foraminifera (Fig. 4B).

Coastal upwelling strengthened during the Bølling, an interpretation supported by multiple proxies. Traditional export productivity proxies, C_{org} (> 2 weight %), and biogenic opal, both increased. Silver transported to sediments by diatoms (Wagner et al., 2013) increased to ~320 ppb (Hendy and Pedersen, 2005) (Fig. 5D). High $\delta^{15}N$ (increasing from ~6 to 8‰) indicates that alongside stronger upwelling there was also increased CU transport of denitrified ETNP water into the shallow (~300 m) California OMZ (Fig. 5B; Hendy et al., 2004). Combined redox and productivity proxies indicate a high oxidant demand from increased export productivity, perhaps stimulated by nutrient-

rich shallow subsurface waters. High export productivity drove low pore water oxygenation during the Bølling consistent with low infaunal I/Ca ratios. However, export productivity subsequently declined during the Allerød (dextral-sinistral *N. pachyderma* ratio increased to ~90%), as C_{org} dropped to glacial values (~1.5%), and Ag concentrations decreased by ~100 ppb (Hendy and Pedersen, 2005) (Figs. 4 and 5). Simultaneously, $\delta^{15}N$ decreased by ~1‰, indicating a reduction in CU transport of denitrified ETP water relative to the Bølling and/or decreased upwelling (Hendy et al., 2004; Hendy and Pedersen, 2005) (Fig. 5B). Taken together, these results imply that sedimentary oxidant demand was relieved during the Allerød due to decline in export production. This diminished oxidant demand is supported by the slight increase in infaunal I/Ca ratios, however these ratios did not return to LGM values (Fig. 5F).

Both infaunal and epifaunal I/Ca ratios were low for ~1000 years through the Allerød indicating that bottom water oxygenation at 950 m water depth declined even as pore water oxidant demand diminished. Relief from sulfidic pore waters is also supported by sedimentary Re enrichments (~10 ppb) (Hendy and Pedersen, 2005) as demonstrated by an increasing Re/Mo ratio (Fig. 4C). Dominance of suboxic benthic foraminifera (35-80%) increased, while the relative abundance of dysoxic and oxic species decreased (Fig. 4F) (Cannariato and Kennett, 1999). Thus the low infaunal and epifaunal I/Ca ratios and high suboxic benthic assemblage abundance must have resulted from decreasing bottom water O_2 concentrations.

The onset of the Younger Dryas is indicated by an abrupt decrease in the dextral-sinistral *N. pachyderma* ratio to <55%. Epifaunal and infaunal I/Ca ratios increase to values similar to the LGM demonstrating both bottom and pore waters once again became oxygenated (Fig. 4F). This observation is supported by a decrease in all redox sensitive metals to minimal values, similar to those between 16-15 ka (Figs. 4 & 5). The I/Br ratio of bulk sediments increased to values >1 indicating loss of IO_3^- from organic matter diminished as pore water O_2 concentrations increased (Hendy and Pedersen, 2005) (Fig. 4B).

5.3 Implications for the evolution of oxygen content of the California Margin

Benthic foraminiferal I/Ca results allow us to determine the relative oxygenation of bottom versus pore water habitats at ODP Hole 1017E, resulting in new insights into the deglacial paleoceanography of the California Margin. We suggest that infaunal I/Ca ratios could be a proxy for export productivity-driven oxidant demand if they are primarily influenced by pore water IO_3^- availability driven by pore water O_2 concentrations. Epifaunal I/Ca ratios on the other hand are a proxy for IO_3^- availability at the SWI, reflecting bottom water O_2 concentrations and thus are a proxy for bottom water mass oxygenation. These interpretations are complicated by our limited understanding of sedimentary iodine digenesis, in addition to the dynamic adaption of benthic foraminifera to food availability and O_2 availability. However, in the eutrophic coastal upwelling environment it is likely to be O_2 that determine the penetration depth of infaunal species

following the TROX-model of Jorissen et al., (1995). Deconvolving bottom water O_2 concentration from pore water oxidant demand is necessary because in the North Pacific the O_2 concentration of subsurface waters changed alongside coastal upwelling intensity and intermediate water production rates in response to ocean-atmospheric reorganization following the last glacial.

Paleoceanographic studies indicate that regional upwelling intensified along the North American margin during warm intervals of the last glacial and deglaciation (Hendy, 2010; Hendy et al., 2004; Ortiz et al., 2004; Schmittner et al., 2007; Pospelova et al., 2015). Primary productivity was greatest at the site during the Bølling and declined through Allerød and Younger Dryas (Hendy et al., 2004; Pospelova et al., 2015) (Fig. 6). High $\delta^{15}N$ values beginning abruptly at the Bølling at multiple sites along the North American Margin imply that the source of upwelled shallow subsurface water (< 300 m) upwelled changed to a low O_2, nutrient-rich denitrified water mass (Hendy et al., 2004; Chang et al, 2008). Simultaneously during the Bølling a shoaling of the OMZ to <350 m is indicated by the dominantly dysoxic benthic foraminiferal response in Santa Barbara Basin (SBB) cores (Ohkushi et al., 2013; Moffit et al., 2015). High export productivity during the Bølling would have increased pore water oxidant demand at ODP Hole 1017E causing infaunal I/Ca ratios to decrease relative to epifaunal ratios. Within the same samples very low infaunal I/Ca ratios are observed while dysoxic benthic foraminifera are present alongside oxic species indicating low pore water O_2 (Figure 4).

While these shallower waters in the CCS indicate a low O_2, nutrient-rich denitrified source, concurrently at 950 m water depth the presence of oxic benthic foraminifera species and epifaunal I/Ca ratios only decrease slightly lower than LGM indicate little change in O_2 concentrations at deep intermediate water depths. Thus the shallower portion of the California OMZ appears poorly oxygenated, while there is only minor decrease in O_2 concentration at the base of the OMZ. This observation can be best explained by a water mass change within the shallow CCS (<300 m) from a northerly sourced well-ventilated glacial mode water similar to winter diffusion of Alaska Gyre water into the North Pacific Current (You et al., 2000) to a poleward flowing denitrified Equatorial subsurface water in the CU (Tetard et al., 2017) (Figure 6D).

Bottom water O_2 concentrations did not decrease at 950 m water depth on the California Margin continental slope until the Allerød, as indicated by very low epifaunal and infaunal I/Ca ratios. At this time primary productivity declined (Pospelova et al., 2015) and $\delta^{15}N$ decreased suggesting weaker upwelling that would have led to diminished sedimentary oxidant demand (Figure 6C; Hendy et al, 2004). However, SBB remained dominantly dysoxic through the Allerød (Ohkushi et al., 2013; Moffitt et al., 2015). The decrease in epifaunal I/Ca ratios at ODP Hole 1017E suggests lower O_2 concentrations at deep intermediate water depths in the CCS. This may have resulted from poorer ventilation of modified NPIW on the California Margin via one or more of the contributing subsurface water masses in the North Pacific

During the Bølling/Allerød, physical changes have been both observed and modeled in NPIW source regions. NPIW production is related to the formation of sea ice in the Okhotsk (Talley, 1991) and Bering seas that diminished as temperatures warmed through deglaciation. During periods of reinvigorated Atlantic Overturning Circulation, decreases in North Pacific salinity resulted in decreased NPIW intrusion into tropical Pacific intermediate layers (Okazaki et al., 2010). However, many studies ascribe reduced O_2 concentrations throughout the OMZ of the North Pacific to productivity changes in the NPIW source regions (Crusius et al., 2004; Lembke-Jene et al., 2017; Praetorius et al., 2015). Specifically, during the Bølling/Allerød high productivity in the Bering Sea is indicated by higher biogenic silica deposition and the presence of the large upwelling diatom species *Chaetoceros* resting and vegetative valves associated with the onset of laminated sediments in the region (Schlung et al., 2013) as well as carbonate maxima (Max et al., 2014). Increased productivity in the Bering Sea has been ascribed to a stronger Bering Slope Current as sea level rose (Kim et al., 2011) in addition to a greater supply of nutrients delivered by glacial meltwater in the Gulf of Alaska (Addison et al., 2012). During the Allerød, Siberian runoff into the Okhotsk Sea fueled productivity diminishing Okhotsk Sea Intermediate Water ventilation (Lembke-Jene et al., 2017). Thus increased oxidant demand at the source of NPIW via enhanced productivity in the western subarctic Pacific could explain lower O_2 concentrations in the water mass without invoking reduced ventilation (Crusius et a., 2004).

Iodate availability at the SWI indicates that bottom water and pore water O_2 concentrations returned to the well ventilated conditions of the last glacial during the YD, in line with other paleoceanographic evidence from the western North American margin (Ohkushi et al., 2013; Chang et al., 2014; Moffit et al., 2015) (Fig. 6B). Pulsed ventilation during the Younger Dryas in the Bering and Okhotsk Seas may have increased the O_2 concentration in NPIW (Max et al., 2014), however primary productivity on the California Margin also decreased during the YD (Pospelova et al., 2015) reducing oxidant demand.

5.4 Future research

Epifaunal and infaunal benthic foraminiferal I/Ca ratios may be used to distinguish relative IO_3^- availability at different sediment depths —from the SWI to 5-10 cm as a qualitative proxy for oxygenation. Further foraminiferal I/Ca has the potential to quantitatively determine past O_2 concentrations if species-specific calibrations are developed. Initial modern calibration studies show a highly significant correlation between bulk I/Ca ratios and bottom water O_2 concentrations despite strong intra-test variability (Glock et al., 2016). Finally, species-specific infaunal I/Ca rations are likely also influenced by changes in microhabitat depth, driven by a combination of sediment O_2 concentrations or food availability (C_{org}), the understanding of which requires more work in modern studies. In combination with the growing suite of stable isotope ratios and multiple element/Ca ratios that can be measured from the same foraminiferal samples such as the Mg/Ca (proxy for ocean temperature), $\delta^{18}O$ (seawater salinity), $\delta^{13}C$ (proxy

for nutrient sources), Mn/Ca (O_2 content), the addition of the I/Ca proxy could improve interpretations of past biogeochemical conditions.

Additionally, iodine pore water chemistry is strongly controlled by particulate organic matter flux and diagenetic recycling of iodine from labile organic matter in addition to the redox state of bottom waters (Kennedy and Elderfield, 1987). Unfortunately, these processes have been little studied since the first pioneering work was undertaken on iodine pore water chemistry (Price and Calvert, 1973; Price and Calvert, 1977; Francois, 1987; Kennedy and Elderfield, 1987). As SWI O_2 concentrations influence diagenetic reactions within sediments based on the redox sequence, future research should focus on understanding the factors that control iodine distribution and speciation at the SWI.

6. CONCLUSION

The foraminiferal species presented in this study make excellent candidates for further calibration studies and demonstrate a history of oxygenation consistent with other well-established proxies. I/Ca ratios from epifaunal, and shallow-to-deep infaunal benthic foraminifera reproduce the IO_3^- availability gradient that tracks O_2 concentration from the sediment-water interface to pore waters.

Thus multi-species benthic I/Ca can be employed to reconstruct the relative contribution of bottom water O_2 and oxidant demand on pore water through time. The I/Ca proxy might enable quantitative reconstruction of O_2 concentrations in both bottom

and pore waters, which could advance understanding of OMZ response to past climate change. By measuring I/Ca ratios from multiple benthic foraminifera species at ODP Hole 1017E we can now demonstrate low O_2 conditions in pore waters during the Bølling (14.7 ka) resulted from high sedimentary oxidant demand driven by increased primary productivity. In contrast, decreased bottom water oxygenation during Allerød was associated with a poorly oxygenated intermediate waters at the base of the OMZ. Well - oxygenated intermediate waters circulated over the site during the LGM and returned during the YD supporting the production of well-ventilated NPIW during cool climate intervals.

ACKNOWLEDGEMENTS

Data presented in this paper will be available on the Pangaea website (http://www.pangaea.de). M.T. was supported with funds from the Geological Society of America and the Scott Turner award through the University of Michigan. A.C. gratefully acknowledges support from the U.S. National Science Foundation (Award # EAR-1503596). Acknowledgment is made to the Donors of the American Chemical Society Petroleum Research Fund, awarded to A.C., for support of this research (ACS-PRF 54583-DNI2)**.** We thank James Kennett and Dorothy Pak for providing samples from the Ocean Drilling Program, sponsored by the United States National Science Foundation. We would like to thank Aurélie Dhenain for help with elemental analyses.

REFERENCES CITED

Addison, J.A., Finney, B.P., Dean, W.E., Davies, M.H., Mix, A.C., Stoner, J.S., and Jaeger, J.M., 2012, Productivity and sedimentary $\delta^{15}N$ variability for the last 17,000 years along the northern Gulf of Alaska continental slope: Paleoceanography, v. 27, no. 1, PA1206.

Altenbach, A.V. and Sarnthein, M., 1989. Productivity record in benthic foraminifera. In: W.H. Berger, V.S. Smetacek and G. Wefer (Editors), Productivity in the Oceans: Present and Past. Wiley, p. 255-269.

Auad, G., 2003, North Pacific Intermediate Water response to a modern climate warming shift: Journal of Geophysical Research, v. 108, no. C11, p. 3349–8.

Cannariato, K.G., and Kennett, J.P., 1999, Climatically related millennial-scale fluctuations in strength of California margin oxygen-minimum zone during the past 60 k.y.: Geology, v. 27, no. 11, p. 975–97.

Chang, A.S., Pedersen, T.F., and Hendy, I.L., 2008, Late Quaternary paleoproductivity history on the Vancouver Island margin, western Canada: a multiproxy geochemical study: Canadian Journal of Earth Sciences, v. 45, no. 11, p. 1283–1297.

Chang, A.S., Pedersen, T.F., and Hendy, I.L., 2014, Effects of productivity, glaciation, and ventilation on late Quaternary sedimentary redox and trace element accumulation on the Vancouver Island margin, western Canada: Paleoceanography, v. 29, p. 730–746.

Chapman, P., and Truesdale, V.W., 2011, Preliminary Evidence for Iodate Reduction in Bottom Waters of the Gulf of Mexico During an Hypoxic Event: Aquatic Geochemistry, v. 17, no. 4-5, p. 671–695.

Chappaz, A., Gobeil, C., and Tessier, A., 2008, Sequestration mechanisms and anthropogenic inputs of rhenium in sediments from Eastern Canada lakes: Geochimica et Cosmochimica Acta, v. 72, no. 24, p. 6027–6036.

Chappaz, A., Lyons, T.W., Gregory, D.D., Reinhard, C.T., Gill, B.C., Li, C., and Large, R.R., 2014, Does pyrite act as an important host for molybdenum in modern and ancient euxinic sediments?: Geochimica et Cosmochimica Acta, v. 126, no. C, p. 112–122.

Chappaz, A., Glass, J.B. and Lyons T.W., in press. Molybdenum. Encyclopedia of Geochemistry, White (ed.), Springer. ISB 978-3-319-39312-4.

Crusius, J., Calvert, S., Pedersen, T., and Sage, D., 1996, Rhenium and molybdenum enrichments in sediments as indicators of oxic, suboxic and sulfidic conditions of deposition: Earth and Planetary Science Letters, p. 65–78.

Crusius, J., Pedersen, T.F., Kienast, S., Keigwin, L., and Labeyrie, L., 2004, Influence of northwest Pacific productivity on North Pacific Intermediate Water oxygen concentrations during the Bølling-Ållerød interval (14.7–12.9 ka): Geology, v. 32, no. 7, p. 633–5.

Diaz, R.J., and Rosenberg, R., 2008, Spreading Dead Zones and Consequences for Marine Ecosystems: Science, v. 321, p. 926–929.

Dyrssen, D., and Kremling, K., 1990, Increasing hydrogen sulfide concentration and trace metal behavior in the anoxic Baltic waters*: Marine Chemistry, v. 30, p. 193–204.

Francois, R., 1987, The influence of humic substances on the geochemistry of iodine in nearshore and hemipelagic marine sediments: Geochimica et Cosmochimica Acta, v. 51, p. 2417–2427.

Glock, N., Liebetrau, V., and Eisenhauer, A., 2014, I/Ca ratios in benthic foraminifera from the Peruvian oxygen minimum zone: analytical methodology and evaluation as a proxy for redox conditions: Biogeosciences, v. 11, no. 23, p. 7077–7095.

Glock, N., Liebetrau, V., Eisenhauer, A., and Rocholl, A., 2016, High resolution I/Ca ratios of benthic foraminifera from the Peruvian oxygen-minimum-zone: A SIMS derived assessment of a potential redox proxy: Chemical Geology, v. 447, p. 40–53.

Hardisty, D.S., Lu, Z., Planavsky, N.J., Bekker, A., Philippot, P., Zhou, X., and Lyons, T.W., 2014, An iodine record of Paleoproterozoic surface ocean oxygenation: Geology, v. 42, no. 7, p. 619–622.

Hardisty, D.S., Lu, Z., Bekker, A., Diamond, C.W., Gill, B.C., Jiang, G., Kah, L.C., Knoll, A.H., Loyd, S.J., Osburn, M.R., Planavsky, N.J., Wang, C., Zhou, X., and Lyons, T.W., 2017, Perspectives on Proterozoic surface ocean redox from iodine contents in ancient and recent carbonate: Earth and Planetary Science Letters, v. 463, p. 159–170.

Hautala, S.L., and Roemmich, D.H., 1998, Subtropical mode water in the Northeast Pacific Basin: Journal of Geophysical Research, v. 103, no. C6, p. 13055 – 13066.

Helz, G.R., and Dolor, M.K., 2012, What regulates rhenium deposition in euxinic basins?: Chemical Geology, v. 304-305, no. C, p. 131–141.

Hendy, I.L., Pedersen, T.F., Kennett, J.P., and Tada, R., 2004, Intermittent existence of a southern Californian upwelling cell during submillennial climate change of the last 60 kyr: Paleoceanography, v. 19, PA3007.

Hendy, I.L., and Pedersen, T.F., 2005, Is pore water oxygen content decoupled from productivity on the California Margin? Trace element results from Ocean Drilling Program Hole 1017E, San Lucia slope, California: Paleoceanography, v. 20, PA4026.

Hendy, I.L., and Pedersen, T.F., 2006, Oxygen minimum zone expansion in the eastern tropical North Pacific during deglaciation: Geophysical Research Letters, v. 33,

no. 20, p. L20602.

Hendy, I.L., 2010, The paleoclimatic response of the Southern Californian Margin to the rapid climate change of the last 60ka: A regional overview: Quaternary International, v. 215, no. 1-2, p. 62–73.

Irino, T., and Pedersen, T.F., 2000, Geochemical character of glacial to interglacial sediments at site 1017, southern Californian margin: Minor and trace elements: Proceedings of the Ocean Drilling Program, Scientific Results, v. 167, p. 263–271.

Jorissen, F. J., de Stigter, H. C. & Widmark, J. G. V., 1995, A conceptual model explaining benthic foraminiferal microhabitats. Marine Micropaleontology 26, 3-15.

Keeling, R.F., Körtzinger, A., and Gruber, N., 2010, Ocean Deoxygenation in a Warming World: Annual Review of Marine Science, v. 2, no. 1, p. 199–229.

Kennedy, H.A., and Elderfield, H., 1987, Iodine diagenesis in pelagic deep-sea sediments: Geochimica et Cosmochimica Acta, v. 51, p. 2489–2504.

Kienast, S.S., Calvert, S.E., and Pedersen, T.F., 2002, Nitrogen isotope and productivity variations along the northeast Pacific margin over the last 120 kyr: Surface and subsurface paleoceanography: Paleoceanography, v. 17, no. 4, p. 7.1–7.17.

Kim, S., Khim, B.K., Uchida, M., Itaki, T., and Tada, R., 2011, Millennial-scale paleoceanographic events and implication for the intermediate-water ventilation in the northern slope area of the Bering Sea during the last 71 kyrs: Global and Planetary Change, v. 79, no. 1-2, p. 89–98.

Lembke-Jene, L., Tiedemann, R., Nurnberg, D., Kokfelt, U., Kozdon, R., Max, L., Röhl, U., and Gorbarenko, S.A., 2017, Deglacial variability in Okhotsk Sea Intermediate Water ventilation and biogeochemistry: Implications for North Pacific nutrient supply and productivity: Quaternary Science Reviews, v. 160, p. 116–137.

Levin, L.A., 2003, Oxygen minimum zone benthos: Adaptation and community response to hypoxia: Oceanography and Marine Biology an Annual Review, v. 41, p. 1–45.

Lynn, R. J., and Simpson, J. J., 1987, The California Current System - The Seasonal Variability Of Its Physical Characteristics: Journal Of Geophysical Research-Oceans, v. 92, no. C12, p. 12947-12966.

Lu, Z., Jenkyns, H.C., and Rickaby, R.E.M., 2010, Iodine to calcium ratios in marine carbonate as a paleo-redox proxy during oceanic anoxic events: Geology, v. 38, no. 12, p. 1107–1110.

Martin, P.A., and Lea, D.W., 2002, A simple evaluation of cleaning procedures on fossil

benthic foraminiferal Mg/Ca: Geochemistry Geophysics Geosystems, v. 3, no. 10, p. 1–8.

Max, L., Lembke-Jene, L., Riethdorf, J.R., Tiedemann, R., Nürnberg, D., Kühn, H., and Mackensen, A., 2014, Pulses of enhanced North Pacific Intermediate Water ventilation from the Okhotsk Sea and Bering Sea during the last deglaciation: Climate of the Past, v. 10, no. 2, p. 591–605.

Middleburg, J.J. and Levin, L.A., 2009, Coastal hypoxia and sediment biogeochemistry: Biogeosciences, v. 6, p. 1273-1293.

Moffitt, S.E., Hill, T.M., Ohkushi, K., Kennett, J.P., and Behl, R.J., 2014, Vertical oxygen minimum zone oscillations since 20 ka in Santa Barbara Basin: A benthic foraminiferal community perspective: Paleoceanography, v. 29, no. 1, p. 44–57.

Moffitt, S.E., Hill, T.M., Roopnarine, P.D., and Kennett, J.P., 2015, Response of seafloor ecosystems to abrupt global climate change: Proceedings of the National Academy of Sciences, v. 112, no. 15, p. 4684–4689.

Nam, S., Takeshita, Y., Frieder, C.A., Martz, T., and Ballard, J., 2015, Seasonal advection of Pacific Equatorial Water alters oxygen and pH in the Southern California Bight: Journal of Geophysical Research: Oceans, v. 120, no. 8, p.

5387–5399.

Noble, M.A., and Ramp, S.R., 2000, Subtidal currents over the central California slope: evidence for offshore veering of the undercurrent and for direct, wind-driven slope currents: Deep-Sea Research Part II, v. 47, p. 871–906.

Ohkushi, K., Kennett, J.P., Zeleski, C.M., Moffitt, S.E., Hill, T.M., Robert, C., Beaufort, L., and Behl, R.J., 2013, Quantified intermediate water oxygenation history of the NE Pacific: A new benthic foraminiferal record from Santa Barbara basin: Paleoceanography, v. 28, no. 3, p. 453–467.

Okazaki, Y., Timmermann, A., Menviel, L., Harada, N., Abe-Ouchi, A., Chikamoto, M.O., Mouchet, A., and Asahi, H., 2010, Deepwater Formation in the North Pacific During the Last Glacial Termination: Science, v. 329, no. 5988, p. 200–204.

Ortiz, J.D., O'Connell, S.B., DelViscio, J., Dean, W., Carriquiry, J.D., Marchitto, T., Zheng, Y., and van Geen, A., 2004, Enhanced marine productivity off western North America during warm climate intervals of the past 52 k.y.: Geology, v. 32, no. 6, p. 521–5.

Pichevin, L.E., Ganeshram, R.S., Francavilla, S., Arellano-Torres, E., Pedersen, T.F., and Beaufort, L., 2010, Interhemispheric leakage of isotopically heavy nitrate in the

eastern tropical Pacific during the last glacial period: Paleoceanography, v. 25, no. 1, p. 368–15.

Pospelova, V., Price, A.M., and Pedersen, T.F., 2015, Palynological evidence for late Quaternary climate and marine primary productivity changes along the California margin: Paleoceanography, v. 30, p. 877–894.

Praetorius, S.K., Mix, A.C., Walczak, M.H., Wolhowe, M.D., Addison, J.A., and Prahl, F.G., 2015, North Pacific deglacial hypoxic events linked to abrupt ocean warming: Nature, v. 527, no. 7578, p. 362–366.

Price, N.B., and Calvert, S.E., 1973, The geochemistry of iodine in oxidised and reduced recent marine sediments: Geochimica et Cosmochimica Acta, v. 37, p. 2149–2158.

Price, N.B., and Calvert, S.E., 1977, The contrasting geochemical behaviours of iodine and bromine in recent sediments from the Namibian shelf: Geochimica et Cosmochimica Acta, v. 41, p. 1769–1775.

Reimer, P. J., et al., 2013, INTCAL13 and MARINE13 radiocarbon age calibration curves 0–50,000 years cal BP: Radiocarbon, v. 55, no. 4, p. 1869–1887.

Reimers, C.E., 1987, An *in situ* microprofiling instrument for measuring interfacial pore water gradients: methods and oxygen profiles from the North Pacific Ocean:

Deep-Sea Research Part I, v. 34, no. 21, p. 2019–2035.

Reimers, C.E., Jahnke, R.A., and McCorkle, D.C., 1992, Carbon fluxes and burial rates over the continental slope and rise off central California with implications for the global carbon cycle: Global Biogeochemical Cycles, v. 6, p. 199–224.

Robinson, S. W., and Thompson, G., 1981, Radiocarbon corrections for marine shell dates with application to southern Pacific Northwest coast prehistory: Syesis, v. 14, p. 45–57.

Rosenthal, Y., Boyle, E.A., Labeyrie, L., and Oppo, D., 1995, Glacial enrichments of authigenic Cd and U in Subantarctic sediments: A climate control on the elements' oceanic budget?: Paleoceanography, v. 10, p. 395–413.

Rue, E.L., Smith, G.J., Cutter, G.A., and Bruland, K.W., 1997, The response of trace element redox couples to suboxic conditions in the water column: Deep-Sea Research Part I, v. 44, p. 113–134.

Schlitzer, R. http://odv.awi.de (2015).

Schmittner, A., Galbraith, E.D., Hostetler, S.W., Pedersen, T.F., and Zhang, R., 2007, Large fluctuations of dissolved oxygen in the Indian and Pacific oceans during Dansgaard-Oeschger oscillations caused by variations of North Atlantic Deep Water subduction: Paleoceanography, v. 22, no. 3, p. PA3207.

Schlung, S.A., Christina Ravelo, A., Aiello, I.W., Andreasen, D.H., Cook, M.S., Drake, M., Dyez, K.A., Guilderson, T.P., LaRiviere, J.P., Stroynowski, Z., and Takahashi, K., 2013, Millennial-scale climate change and intermediate water circulation in the Bering Sea from 90 ka: A high-resolution record from IODP Site U1340: Paleoceanography, v. 28, no. 1, p. 54–67.

Scott, C., and Lyons, T.W., 2012, Contrasting molybdenum cycling and isotopic properties in euxinic versus non-euxinic sediments and sedimentary rocks: Refining the paleoproxies: Chemical Geology, v. 324-325, no. C, p. 19–27.

Stramma, L., Johnson, G.C., Sprintall, J., and Mohrholz, V., 2008, Expanding oxygen-minimum zones in the tropical oceans: Science, v. 320, no. 5876, p. 655–658.

Tada, R., Sato, S., Irino, T., Matsui, H., and Kennett, J.P., 2000, Millennial-scale compositional variations in late quaternary sediments at site 1017, Southern California: Proceedings of the Ocean Drilling Program, Scientific Results, v. 167, p. 277–296.

Talley, L.D., 1991, An Okhotsk Sea water anomaly: implications for ventilation in the North Pacific: Deep Sea Research, v. 38, Suppl 1, p. S171–S190.

Tetard, M., Licari, L., and Beaufort, L., 2017, Oxygen history off Baja California over the last 80 kyr: A new foraminiferal proxy record of benthic oxygenation: Paleoceanography, v. 379, p.

243–19.

Wagner, M., Hendy, I.L., McKay, J.L., and Pedersen, T.F., 2013, Influence of biological productivity on silver and redox-sensitive trace metal accumulation in Southern Ocean surface sediments, Pacific sector: Earth and Planetary Science Letters, v. 380, no. C, p. 31–40.

Wagner, M., Hendy, I.L., McKay, J.L., and Pedersen, T.F., 2015, Redox chemistry of West Antarctic Peninsula margin surface sediments: Chemical Geology, v. 417, p. 102–114.

Whitney, F.A., Freeland, H.J., and Robert, M., 2007, Persistently declining oxygen levels in the interior waters of the eastern subarctic Pacific: Progress In Oceanography, v. 75, no. 2, p. 179–199.

You, Y., Suginohara, N., Fukasawa, M., Yasuda, I., Kaneko, I., Yoritaka, H., and Kawamiya, M., 2000, Roles of the Okhotsk Sea and Gulf of Alaska in forming the North Pacific Intermediate Water: Journal of Geophysical Research: Biogeosciences, v. 105, p. 3253–3280.

You, Y., 2003, The pathway and circulation of North Pacific Intermediate Water: Geophysical Research Letters, v. 30, no. 24, p. 2291.

Zhou, X., Thomas, E., Rickaby, R.E.M., Winguth, A.M.E., and Lu, Z., 2014, I/Ca

evidence for upper ocean deoxygenation during the PETM: Paleoceanography, v. 29, no. 10, p. 964–975.

Zhou, X., Jenkyns, H.C., Owens, J.D., Junium, C.K., Zheng, X.-Y., Sageman, B.B., Hardisty, D.S., Lyons, T.W., Ridgwell, A., and Lu, Z., 2015, Upper ocean oxygenation dynamics from I/Ca ratios during the Cenomanian-Turonian OAE 2: Paleoceanography, v. 30, no. 5, p. 510–526.

Zhou, X., Thomas, E., Winguth, A.M.E., Ridgwell, A., Scher, H., Hoogakker, B.A.A., and Lu, Z., 2016, Expanded oxygen minimum zones during the late Paleocene-early Ecocene: Hints from mulitproxy comparison and ocean modeling: Paleoceanography, v. 31, p. 1532 – 1546.

FIGURE CAPTIONS

Figure 1. A) Map of North Pacific Ocean showing location of ODP Hole 1017E on the Santa Lucia slope, California (34˚32'N: 121°60'W, 955 m water depth). B) Water column profile of dissolved O_2 concentration for a northeastern Pacific transect (Schlitzer, 2015, Ocean Data View). The modern bottom water O_2 concentration for ODP Hole 1017E indicated by an x, while dashed lines separate oxic and suboxic water.

Figure 2. Benthic foraminiferal I/Ca ratios of A) epifanual *Cibicidoides* sp. (diamonds and dashed line), B) shallow infaunal *Uvigerina peregrina* (red squares and solid red line) and C) deep infaunal *Bolivina spissa* (circles and solid black line). Thick lines represent the average of all analyses binned into 4 time intervals: the LGM, the Bølling, the Allerød, and the YD. Major warm interstadials through the last deglaciation are shaded and the defined oxygen concentrations from oxic to dysoxic conditions are labeled.

Figure 3. Schematic representation of depth habitats expected for multiple benthic species and diagenetic processes controlling IO_3^- and I^- distributions in pore water under different redox conditions (adapted from Kennedy and Elderfield, 1987). A)

Representation of a benthic environment with low sedimentary C_{org} under well oxygenated bottom water. B) The Last Glacial Maximum; bottom water is oxygenated, sedimentary C_{org} is low. C) The Bølling; bottom water is oxygenated, sedimentary C_{org} production is high and D) the Allerød; bottom water is oxygenated-depleted. Three benthic foraminifera are shown: Epifaunal (*Cibicidoides sp.*), shallow infaunal (*Uvigerina sp)*, and deep infaunal (*Bolivina sp.*). Pore water IO_3^- (solid line) and I^- (dashed line) ion concentrations are displayed over relative pore water oxygenation and C_{org} concentration. 1. I^- production at the sediment water interface (SWI), 2. I^- oxygenation in oxic pore waters, 3. IO_3^- reduction in suboxic pore waters and 4. I^- production from IO_3^- associated C_{org}.

Figure 4. Comparison of different redox proxy records associated with bottom and pore water oxygenation from ODP Hole 1017E versus calendar age BP (ka). A) I/Ca ratio for *Cibicidoides sp.* (diamonds and dashed line), *U. peregrina* (red squares and solid red line), deep infaunal *Bolivina spissa* (circles and solid black line), where thick lines represent the average of all analyses binned by sample depths falling within the following intervals: the LGM, the Bølling, the Allerød, and the YD;.B) bulk sediment I/Br ratio (Hendy and Pedersen, 2005); C) bulk sediment Re concentration (ppb; dashed line) (Hendy and Pedersen, 2005); D) bulk sediment Mo concentration (ppm) (Hendy and Pedersen, 2005);

E) Re/Mo ratio (dashed line); F) benthic foraminiferal assemblage, percentages grouped into dysoxic (dark gray shading), suboxic 1 (gray shading), suboxic 2 (light gray shading), and oxic indicators (black shading) (Cannariato and Kennett, 1999). Major warm interstadials through the last deglaciation are shaded and the defined O_2 concentrations from oxic to dysoxic conditions are labeled.

Figure 5. Comparison of productivity proxy records with bottom and pore water oxygenation from ODP Hole 1017E versus calendar age BP (ka). A) The ratio of dextral to sinistral *N. pachyderma* indicating timing of climate events (Hendy, 2010); B) $\delta^{15}N$ of organic matter (Hendy et al., 2004); C) total organic carbon (weight %) (Irino and Pedersen, 2000); D) bulk sediment silver concentration (ppb) (Hendy and Pedersen, 2005); E) bulk sediment cadmium concentration (ppm) (Hendy and Pedersen, 2005); and F) I/Ca ratios standardized to the mean value of all samples for *Cibicidoides sp.* (dashed line), *U. peregrina* (solid red line), and *B. spissa* (solid black line). Major warm interstadials through the last deglaciation are shaded.

Figure 6. Schematic of shallow subsurface water characteristics on the California Margin during the late glacial. The depth and locations of ODP Hole 1017E (San Lucia Slope), ODP Site 893 (Santa Barbara Basin), and MV0811-15JC (Santa Barbara Basin slope) relative to water masses are indicated for the following time intervals A. present day; B.

Younger Dryas; C. Allerød; D. Bølling; and E. the Late Glacial. Decreasing O_2 concentrations in water masses indicated by depth of orange shading, while relative primary productivity indicated by number and thickness of green lines. The following water mass abbreviations are used; California Undercurrent (CU), Eastern Subtropical Subsurface Water (ESsW), North Pacific Intermediate Water (NPIW) and Pacific Deep Water (PDW).

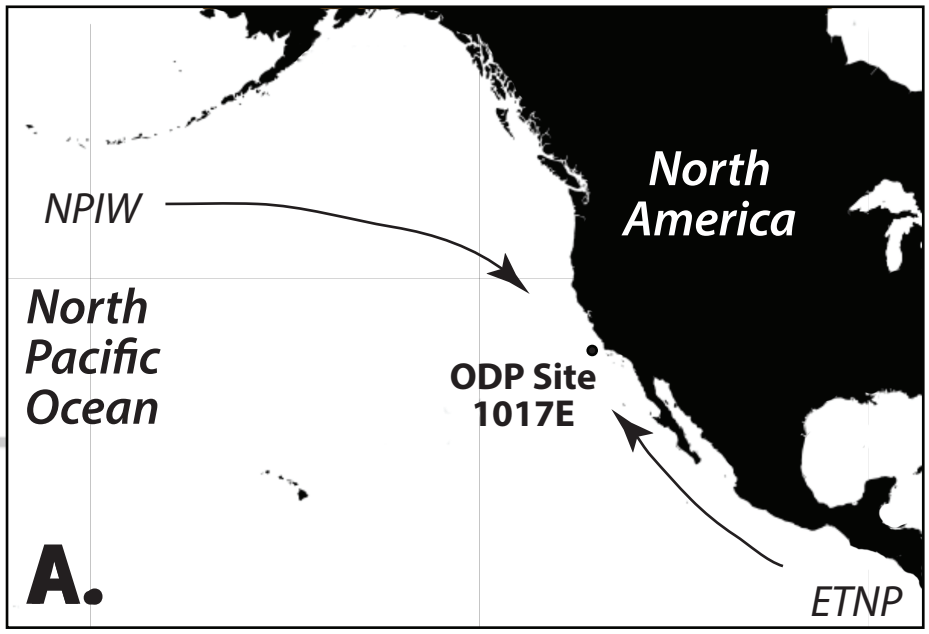

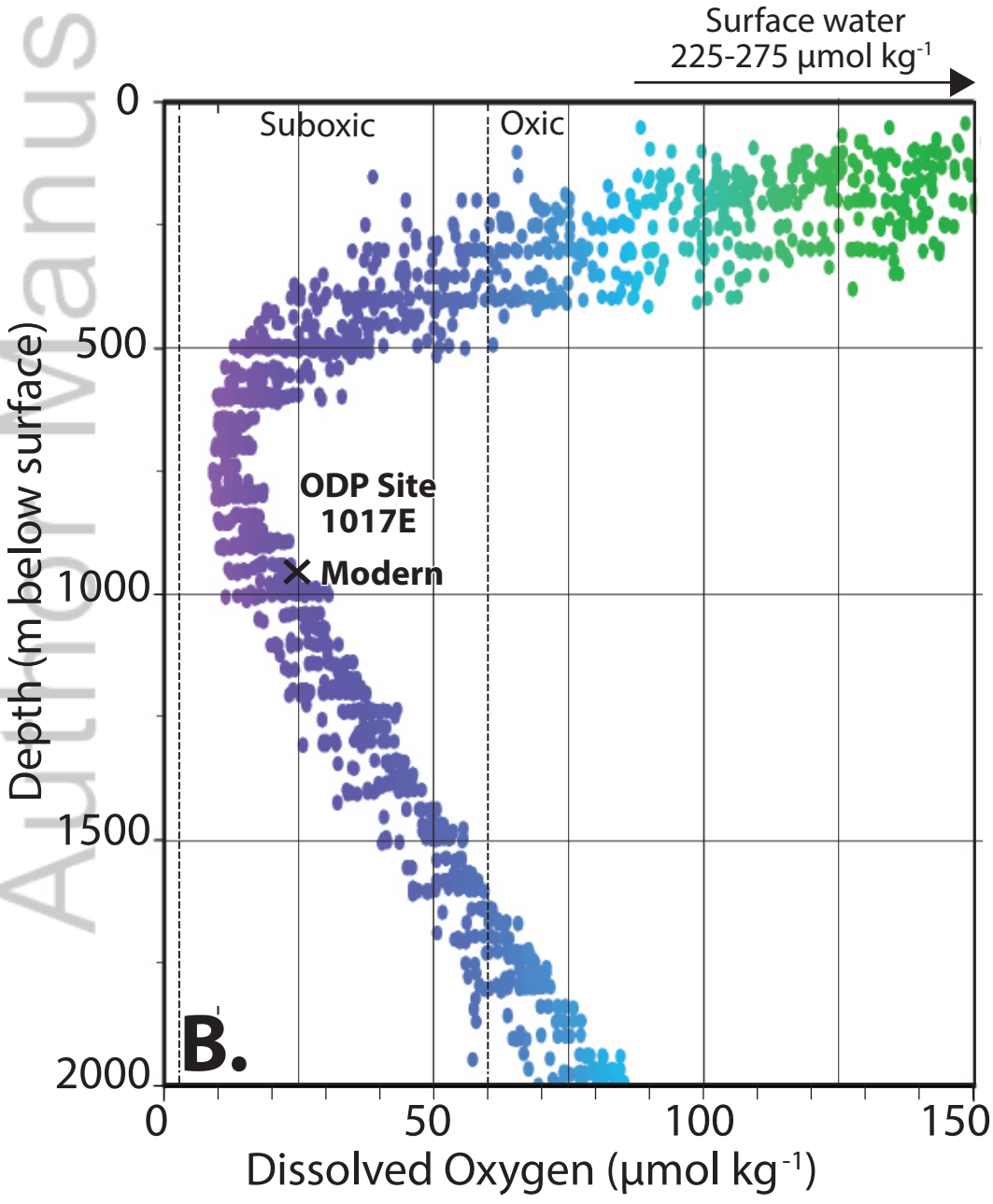

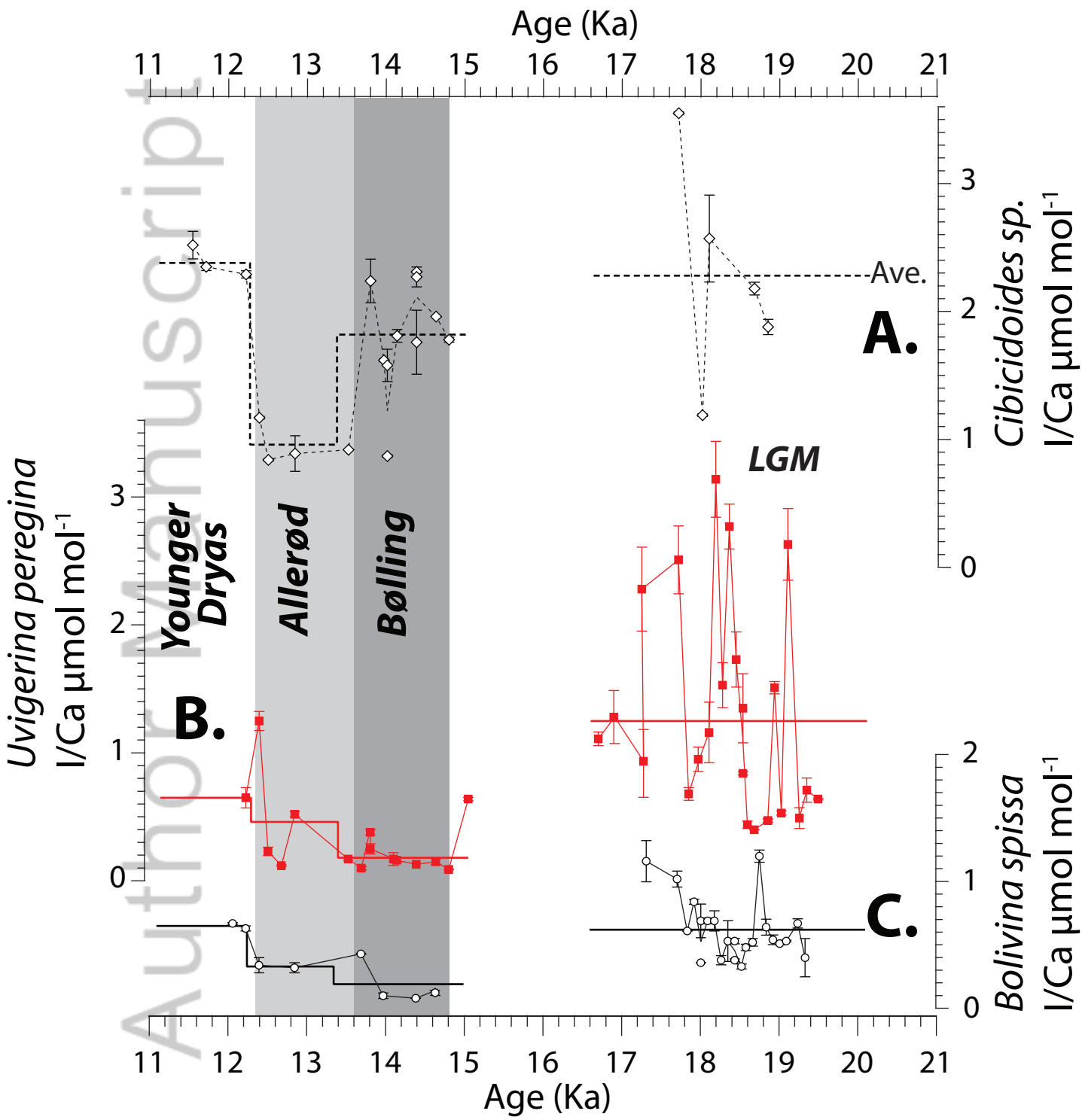

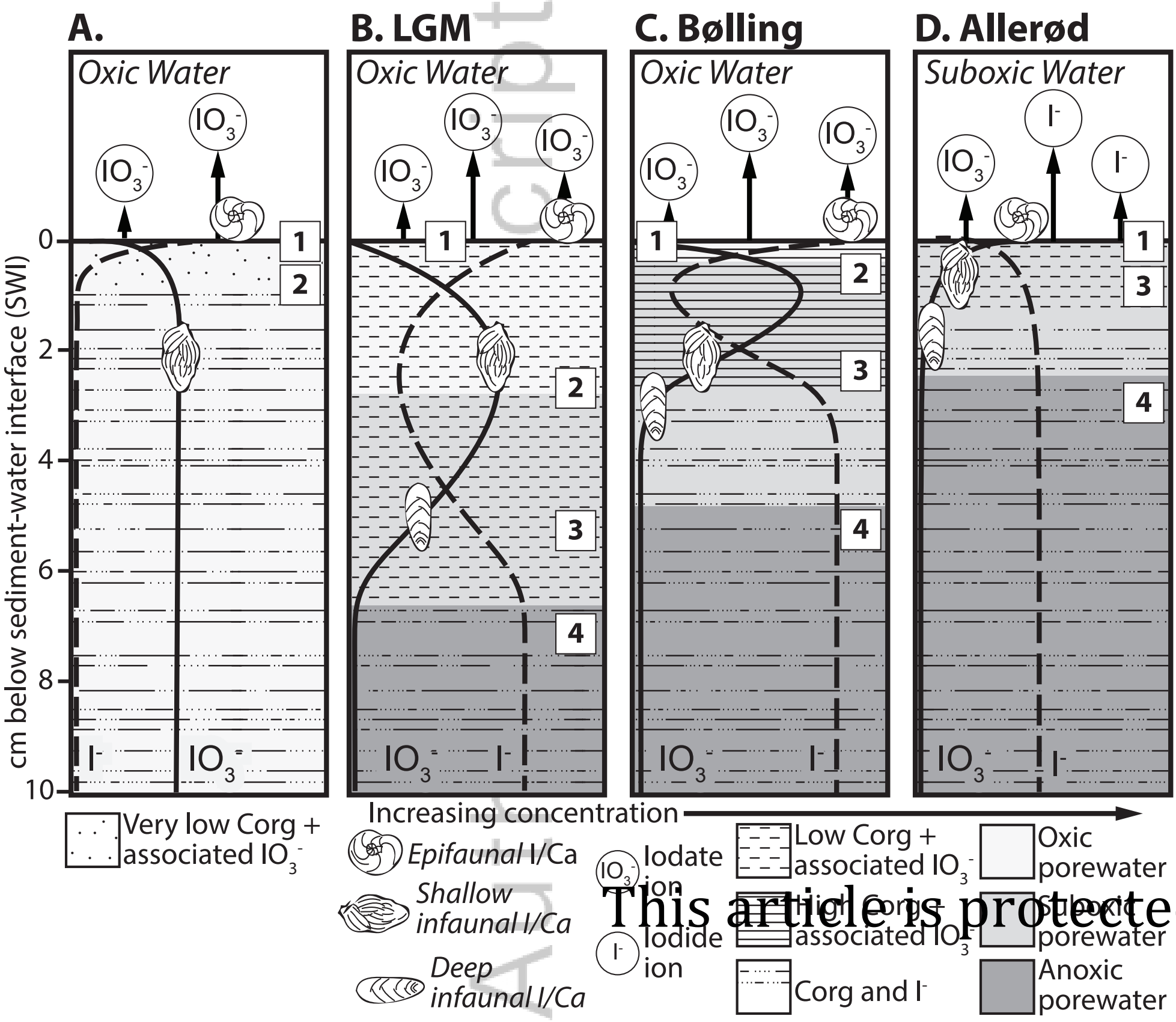

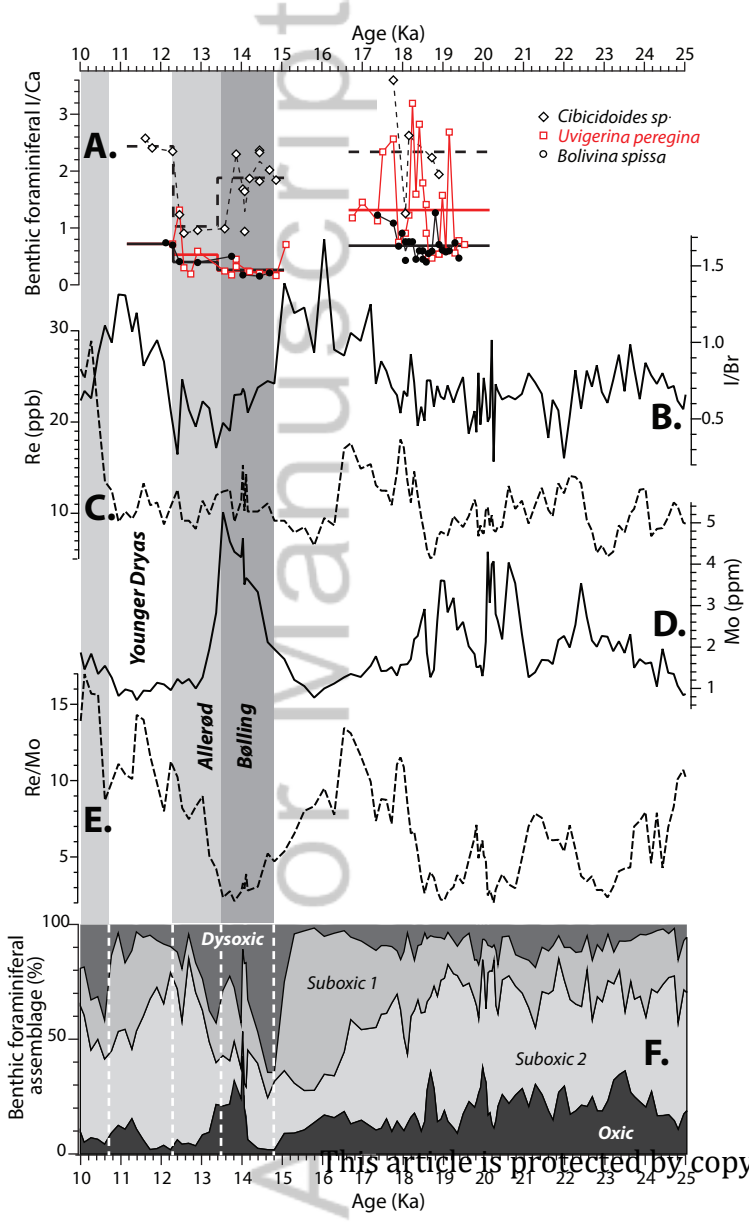

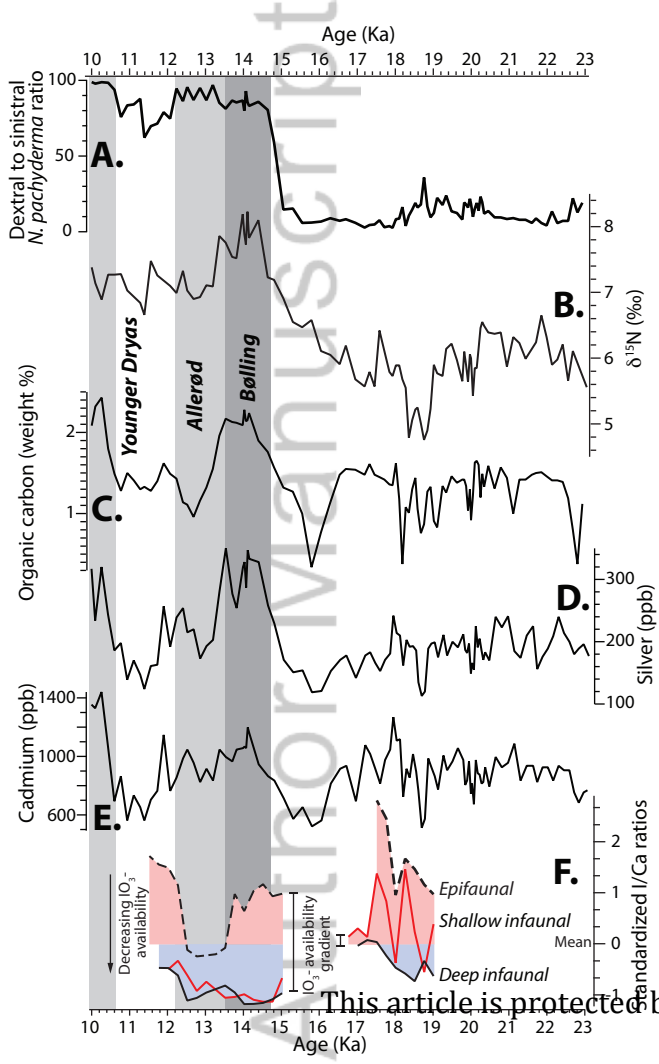

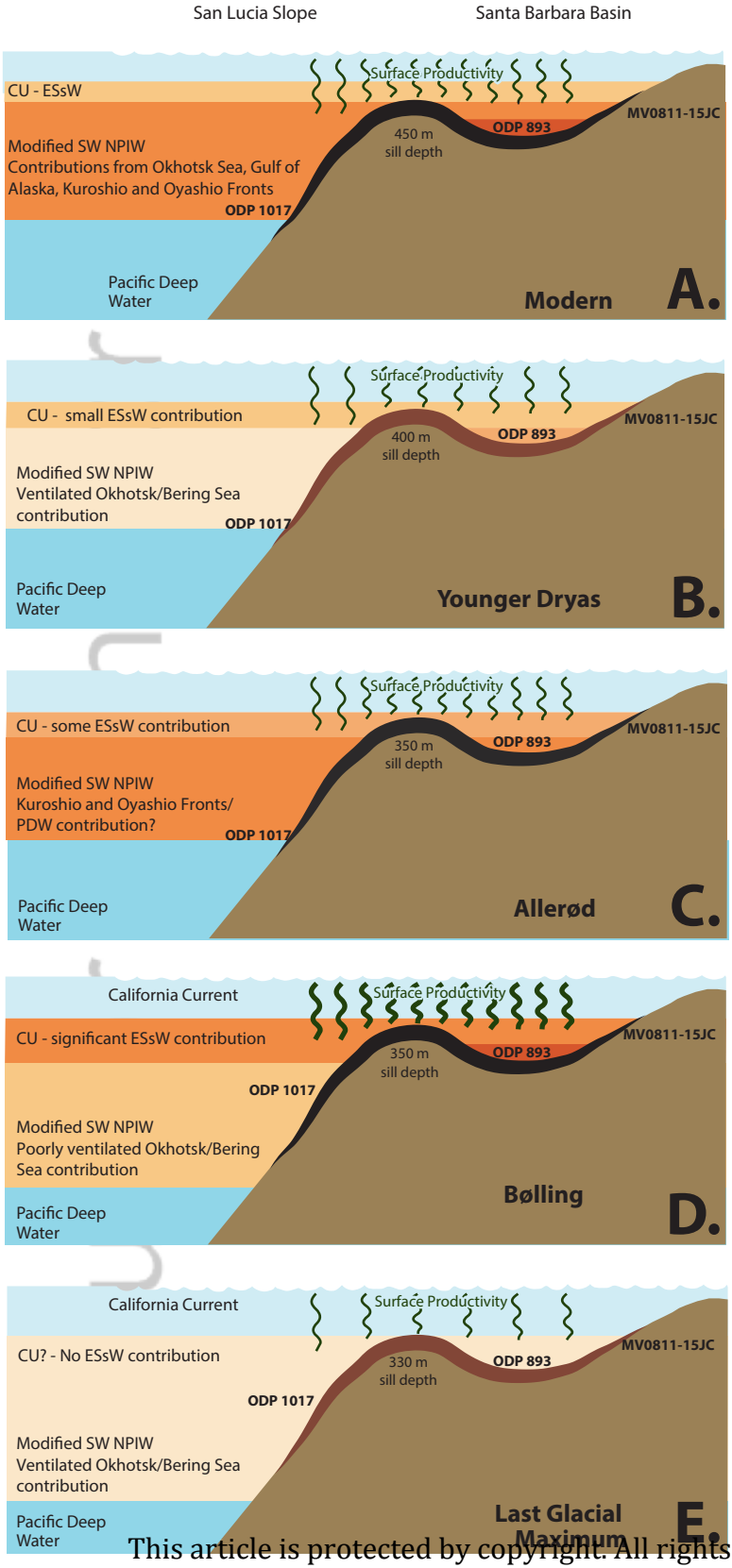

Hendy Ingrid (Orcid ID: 0000-0001-8305-6752)

Table 1. Element concentrations and volumes of pre-dilutions for ICP-MS standards.

Standard or dilution	Ca (ppm)	Iodine	25% TMAH (µL)	1000 ppm Ca (µL)	Iodine pre-dilution (µL)	2% HNO3 (mL)	Concentration of iodine pre-dilution
10 ppm I	0	10 ppm	300	0	150	14.550	1000 ppm I
100 ppb I	0	100 ppb	300	0	150	14.550	10 ppm I
10 ppb I	0	10 ppb	300	0	1500	13.200	100 ppb I
Standard 1	50	1000 ppt	300	750	150	13.800	100 ppb I
Standard 2	50	500 ppt	300	750	75	13.875	100 ppb I
Standard 3	50	250 ppt	300	750	37.5	13.913	100 ppb I
Standard 4	50	100 ppt	300	750	150	13.800	10 ppb
Standard 5	50	50 ppt	300	750	75	13.875	10 ppb
Standard 6	50	25 ppt	300	750	37.5	13.913	10 ppb
Blank	50	0 ppt	300	750	0	13.950	-

Hendy Ingrid (Orcid ID: 0000-0001-8305-6752)

Table 2. Elemental concentrations and relative standard deviation for sample and internal reference standard measurements

Sample ID	Core	Corrected depth (m)	Species	Number of foraminifera	Sample weight (µg)	Ca (ppm)	RSD (%)	Y (%)	I (ppt)	RSD (%)	Y (%)	Y RSD (%)
1	1017E 1H 2	2.91	*Cibicidoides sp.*	3	370	41	2.1	104	120	1.3	92	1.5
2	1017E 1H 2	2.91	*U. peregrina*	4	388	45	0.7	106	24	7.6	86	0.3
3 **	1017E 1H 2	2.91	*B. spissa*	9	200	19	1.6	107	379	2.6	90	0.2
5 *	1017E 1H 2	2.94	*U. peregrina*	4	278	31	6.0	105	9	3.4	84	4.1
6	1017E 1H 2	2.94	*B. spissa*	10	172	19	0.3	106	25	1.8	89	1.2
7	1017E 1H 2	2.97	*Cibicidoides sp.*	4	344	22	2.2	107	156	9.9	95	1.3
8 *	1017E 1H 2	2.97	*U. peregrina*	3	242	44	0.6	105	38	1.5	86	0.5
10	1017E 1H 3	3.00	*Cibicidoides sp.*	4	312	49	1.1	107	252	1.9	94	1.3
12 *	1017E 1H 3	3.00	*B. spissa*	10	186	36	2.1	106	9	2.6	86	1.9
13	1017E 1H 2	2.97	*U. peregrina*	3	242	22	1.5	104	27	7.0	89	1.9
14	1017E 1H 3	3.03	*Cibicidoides sp.*	3	234	39	0.7	105	109	1.6	85	4.2
16	1017E 1H 3	3.09	*U. peregrina*	5	378	53	0.7	106	28	13.8	92	3.8
17	1017E 1H 3	3.12	*Cibicidoides sp.*	3	178	26	0.4	103	148	3.1	84	1.1
18	1017E 1H 3	3.12	*U. peregrina*	5	444	51	0.6	104	26	11.2	89	2.2
20	1017E 1H 3	3.15	*Cibicidoides sp.*	3	380	64	18.6	102	355	1.6	91	1.0
22	1017E 1H 3	3.15	*B. spissa*	15	378	61	1.0	105	16	4.4	92	0.8
23	1017E 1H 3	3.18	*Cibicidoides sp.*	4	306	53	1.1	103	328	1.0	99	1.9
24	1017E 1H 3	3.18	*U. peregrina*	4	336	51	1.2	103	23	10.3	93	1.4
25 *	1017E 1H 3	3.18	*B. spissa*	10	318	31	4.7	103	12	1.2	100	1.7
26	1017E 1H 3	3.21	*Cibicidoides sp.*	3	254	18	1.6	105	103	2.2	97	1.4
27	1017E 1H 3	3.21	*U. peregrina*	4	466	78	7.7	104	23	6.4	96	1.0
28	1017E 1H 3	3.03	*Cibicidoides sp.*	3	234	30	9.8	105	152	1.0	91	1.5
30	1017E 1H 3	3.15	*U. peregrina*	3	248	56	0.9	102	23	6.4	91	1.5
31	1017E 1H 2	2.79	*Cibicidoides sp.*	3	208	6	0.1	106	16	14.0	80	0.6
32	1017E 1H 2	2.79	*U. peregrina*	3	247	22	8.6	104	37	13.0	98	0.7
33	1017E 1H 2	2.79	*B. spissa*	22	204	16	2.2	100	17	12.5	87	0.9
35	1017E 1H 2	2.76	*U. peregrina*	4	350	46	1.0	102	17	7.1	83	0.4
37	1017E 1H 2	2.73	*Cibicidoides sp.*	3	220	52	2.1	116	140	0.9	81	0.4
38 *	1017E 1H 2	2.73	*U. peregrina*	4	288	55	3.3	106	36	2.1	98	2.2
40	1017E 1H 2	2.70	*Cibicidoides sp.*	3	240	35	1.4	103	131	2.5	85	0.1
42	1017E 1H 2	2.70	*U. peregrina*	4	298	47	2.7	101	184	8.8	90	0.7
43	1017E 1H 2	2.70	*B. spissa*	15	128	13	1.5	103	14	12.4	89	1.1
44	1017E 1H 2	2.67	*Cibicidoides sp.*	4	198	28	2.6	104	199	1.4	83	1.8
45	1017E 1H 2	2.67	*U. peregrina*	4	402	49	1.4	99	99	13.9	89	6.7
46	1017E 1H 2	2.67	*B. spissa*	15	288	16	1.3	100	33	3.1	85	2.1
49	1017E 1H 2	2.64	*B. spissa*	20	158	20	1.4	101	43	1.7	94	0.8
53	1017E 1H 2	2.58	*Cibicidoides sp.*	3	180	22	1.7	101	167	3.3	90	0.6
55	1017E 1H 2	2.55	*Cibicidoides sp.*	3	214	30	5.9	103	236	1.4	93	0.5
61	1017E 1H 3	3.57	*U. peregrina*	4	418	32	5.5	101	232	10.8	88	0.5
62 *	1017E 1H 3	3.54	*U. peregrina*	3	308	47	1.4	103	132	3.1	86	3.9
63	1017E 1H 3	3.54	*B. spissa*	15	240	25	0.5	100	90	14.7	83	0.6
64 *	1017E 1H 3	3.48	*U. peregrina*	3	316	52	0.5	102	209	2.2	90	1.3
65	1017E 1H 3	3.90	*U. peregrina*	3	327	62	0.7	102	164	2.2	86	4.2
66	1017E 1H 3	3.90	*B. spissa*	20	248	35	1.2	103	37	4.9	92	0.8
67	1017E 1H 3	3.87	*U. peregrina*	3	320	60	0.4	102	326	13.0	80	1.8
68	1017E 1H 3	3.87	*B. spissa*	15	260	44	1.4	101	53	4.1	84	1.0
69	1017E 1H 3	3.84	*U. peregrina*	3	336	66	0.6	100	579	7.1	91	2.7
70 *	1017E 1H 3	3.84	*B. spissa*	20	184	27	6.2	100	47	3.5	87	0.8
71	1017E 1H 3	3.81	*U. peregrina*	3	346	63	0.9	100	304	12.6	80	2.8
72	1017E 1H 3	3.81	*B. spissa*	15	336	28	1.5	100	34	9.7	95	0.8
73	1017E 1H 3	3.90	*U. peregrina*	3	327	60	0.3	101	255	11.6	83	4.4
74	1017E 1H 3	3.78	*U. peregrina*	3	374	74	1.1	102	735	10.7	112	0.7
75	1017E 1H 3	3.78	*B. spissa*	15	252	47	0.4	102	103	12.2	105	3.6

Table 2. Continued

Sample ID	Core	Corrected depth (m)	Species	Number of foraminifera	Sample weight (µg)	Ca (ppm)	RSD (%)	Y (%)	I (ppt)	RSD (%)	Y (%)	Y RSD (%)
77	1017E 1H 3	3.75	*U. peregrina*	3	328	65	0.7	101	237	13.8	87	0.9
78	1017E 1H 3	3.75	*B. spissa*	19	204	37	0.5	101	81	4.4	100	0.8
79	1017E 1H 3	3.72	*Cibicidoides sp.*	3	228	35	5.3	100	133	5.8	84	2.5
80 *	1017E 1H 3	3.72	*U. peregrina*	3	322	34	5.9	95	98	3.6	81	1.1
81 *	1017E 1H 3	3.72	*B. spissa*	15	224	17	1.6	100	32	3.3	92	1.0
83	1017E 1H 3	3.69	*B. spissa*	15	198	28	0.4	102	74	1.9	92	0.3
84	1017E 1H 3	3.66	*U. peregrina*	3	318	64	1.8	101	138	9.3	108	1.3
85	1017E 1H 3	3.87	*B. spissa*	15	260	27	0.7	103	45	4.6	95	5.2
86	1017E 1H 3	3.66	*B. spissa*	15	268	51	1.2	103	99	1.1	106	0.9
87	1017E 1H 3	3.63	*Cibicidoides sp.*	3	130	20	1.2	100	226	0.9	97	0.4
88	1017E 1H 3	3.63	*U. peregrina*	3	380	72	1.4	101	570	12.2	104	2.5
89	1017E 1H 3	3.63	*B. spissa*	15	188	26	0.5	101	85	7.2	97	0.3
90	1017E 1H 3	3.72	*B. spissa*	15	224	33	6.2	102	37	6.1	85	1.1
91	1017E 1H 3	4.20	*U. peregrina*	3	376	58	1.0	101	117	2.0	82	0.3
94 *	1017E 1H 3	4.17	*U. peregrina*	3	316	58	1.3	101	163	2.1	89	2.3
96 *	1017E 1H 3	4.14	*U. peregrina*	3	382	57	0.4	101	81	3.4	103	1.8
97	1017E 1H 3	4.14	*B. spissa*	20	310	38	1.6	102	80	6.9	93	1.3
98	1017E 1H 3	4.11	*U. peregrina*	3	388	58	0.5	102	481	11.2	103	1.1
99	1017E 1H 3	4.11	*B. spissa*	15	306	44	0.3	102	73	1.8	85	0.6
100	1017E 1H 3	4.08	*U. peregrina*	3	360	66	0.4	101	111	3.6	89	2.5
101	1017E 1H 3	4.08	*B. spissa*	15	282	33	5.4	101	53	4.2	86	0.7
102	1017E 1H 3	4.05	*U. peregrina*	3	250	36	0.4	103	171	3.5	84	2.4
103	1017E 1H 3	4.05	*B. spissa*	20	308	50	1.1	101	86	7.5	84	2.2
104	1017E 1H 3	4.02	*Cibicidoides sp.*	3	196	26	1.1	102	156	4.2	87	0.9
105	1017E 1H 3	4.02	*U. peregrina*	3	330	44	0.1	102	65	2.4	87	2.9
106	1017E 1H 3	4.02	*B. spissa*	15	366	22	0.5	102	44	10.7	84	0.6
108	1017E 1H 3	3.99	*B. spissa*	15	192	27	0.3	102	101	3.9	89	1.5
109	1017E 1H 3	4.17	*B. spissa*	15	218	30	0.7	101	37	4.7	90	0.8
110	1017E 1H 3	3.96	*Cibicidoides sp.*	3	240	30	1.2	101	204	3.5	97	0.7
111	1017E 1H 3	3.96	*U. peregrina*	3	386	65	0.6	100	83	0.6	87	1.4
112	1017E 1H 3	3.96	*B. spissa*	15	176	27	1.7	99	45	7.3	85	0.7
113	1017E 1H 3	3.93	*U. peregrina*	3	284	55	1.2	101	76	7.6	86	2.1
114	1017E 1H 3	3.93	*B. spissa*	15	212	37	0.4	101	55	6.2	86	1.5
115	1017E 1H 3	3.45	*U. peregrina*	3	314	45	1.0	100	159	5.8	87	3.8
117	1017E 1H 3	3.24	*U. peregrina*	3	236	45	0.7	100	90	2.9	87	1.2
118	1017E 1H 3	3.15	*Cibicidoides sp.*	3	260	51	1.8	101	374	1.5	93	1.0
119	1017E 1H 3	4.02	*U. peregrina*	3	330	59	2.0	101	88	5.1	82	2.7
120	1017E 1H 3	3.15	*Cibicidoides sp.*	3	260	36	6.4	101	256	2.8	82	1.7

*** Indicates third and last scan removed due to insufficient sample**

**** Indicates outlier, >3σ**

Hendy Ingrid (Orcid ID: 0000-0001-8305-6752)

Table 3. Quality controls for standards (I and Ca), and percent recovery of the internal standard (Y)

Controls	I (ppt)	Ca (ppb)	Y (%)
I 50 ppt	53		97
I 50 ppt	50		98
I 50 ppt	52		99
I 50 ppt	51		98
I 100 ppt	105		102
I 100 ppt	105		101
I 100 ppt	102		101
I 100 ppt	99		102
I 200 ppt	192		96
I 200 ppt	198		101
I 200 ppt	203		100
I 200 ppt	197		103
Ca 250 ppb		241	96
Ca 250 ppb		252	98
Ca 250 ppb		244	101
Ca 250 ppb		247	96
Ca 500 ppb		508	97
Ca 500 ppb		502	98
Ca 500 ppb		512	96
Ca 500 ppb		509	100
Ca 750 ppb		756	98
Ca 750 ppb		767	96
Ca 750 ppb		762	101
Ca 750 ppb		753	99
Ca 1000 ppb		1014	95
Ca 1000 ppb		1023	99
Ca 1000 ppb		1007	102
Ca 1000 ppb		1021	97